

1 Article

2 

# Methylation-based reclassification of bladder cancer 3 based on immune cell genes

4 Qizhan Luo <sup>1</sup>, and Thomas-Alexander Vögeli <sup>1,\*</sup>5 <sup>1</sup> Department of Urology, RWTH Aachen University, Pauwelsstrasse 30, 52072 Aachen, Germany;  
6 [qizhan.luo@rwth-aachen.de](mailto:qizhan.luo@rwth-aachen.de)(Q.L.); [tvoegeli@ukaachen.de](mailto:tvoegeli@ukaachen.de)(T-A.V.)7 \* Correspondence: [tvoegeli@ukaachen.de](mailto:tvoegeli@ukaachen.de)

8

9 **Simple Summary:** Bladder cancer (BC) development is highly related to immune cell infiltration  
10 and inflammation. This study aimed to construct a new classification of bladder cancer (BC)  
11 molecular subtypes based on immune cells-associated CpG sites. The classification was accurate  
12 and stable. BC patients could be divided into three subtypes based on the immune cells-associated  
13 CpG sites. The distribution of immune cells, level expression of checkpoints, stromal score, immune  
14 score, ESTIMATEScore, tumor purity, APC\_co\_inhibition, APC\_co\_stimulation, HLA,  
15 MHC\_class\_I, Type\_I\_IFN\_Reponse, and Type\_II\_IFN\_Reponse were significant difference among  
16 three subgroups. The distribution of genomic alterations was different among them. High level  
17 immune infiltration was a correlation with high level methylation. The lower RNAss score was  
18 associated with higher immune infiltration and higher level expression of CD274.19 **Abstract:** Background: Bladder cancer (BC) development is highly related to immune cell  
20 infiltration and inflammation. This study aimed to construct a new classification of bladder cancer  
21 (BC) molecular subtypes based on immune cells-associated CpG sites. Methods: The genes of 28  
22 types of immune cells were obtained from previous studies. Then methylation sites corresponding  
23 to immune cells-associated genes were acquired. Differentially methylation sites (DMSs) were  
24 identified between normal samples and bladder cancer samples. Unsupervised clustering analysis  
25 of differentially methylation sites was performed to divide into several subtypes. Then the potential  
26 mechanism of different subtypes was exploded. Result: Bladder cancer patients were divided into  
27 three groups. Cluster 3 (methylation-L) subtype had the best prognosis. Cluster 1 (methylation-M)  
28 had the worst prognosis. The distribution of immune cells, level expression of checkpoints, stromal  
29 score, immune score, ESTIMATEScore, tumor purity, APC\_co\_inhibition, APC\_co\_stimulation,  
30 HLA, MHC\_class\_I, Type\_I\_IFN\_Reponse, and Type\_II\_IFN\_Reponse were significant difference  
31 among three subgroups. The distribution of genomic alterations was different among them.  
32 Conclusion: The classification was accurate and stable. BC patients could be divided into three  
33 subtypes based on the immune cells-associated CpG sites. Specific biological signaling pathways,  
34 immune mechanisms, and genomic alterations were various among three subgroups. High level  
35 immune infiltration was a correlation with high level methylation. The lower RNAss score was  
36 associated with higher immune infiltration and higher level expression of CD274.37 **Keywords:** Immune cell; DNA CpGs; Bladder cancer; Subtype; mutation; CNV; Immune score;  
38 Immune Checkpoints

39

40 

## 1. Introduction

41 Recently, diverse immunotherapy has been proven to successfully treat numerous lethal  
42 cancers[1]. These included cytokine treatment, cellular therapy, immune checkpoint blockade, and

43 therapeutic vaccines[2]. Immune checkpoint inhibitors have shown remarkable anti-tumor function  
44 in several human cancers, including programmed cell death protein 1 (PD-1), cytotoxic T lymphocyte  
45 antigen-4 (CTLA-4), and PD-1 ligand (PD-L1) antibodies[3-5]. FDA approved two cytokines as anti-  
46 tumor agents against kidney malignancy and metastatic melanoma[6]. Preventive and therapeutic  
47 vaccines have a significant anti-tumor function in several cancers, such as hepatitis B virus  
48 vaccines[7], Sipuleucel-T, human papillomavirus[8], and GVAX vaccine against prostate cancer[9,  
49 10]. However, there is heterogeneity in response rates, and not all immunotherapy is successful in  
50 treating patients[11].

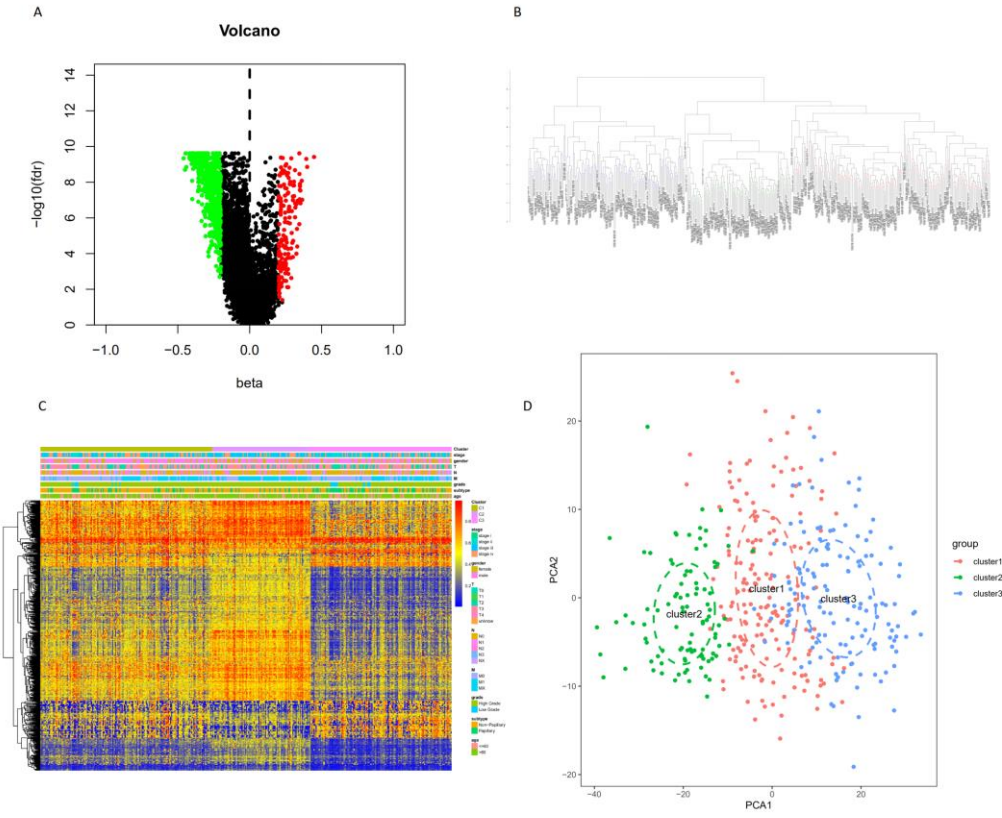
51 BC development is highly related to immune cell infiltration and inflammation. A previous  
52 study also revealed the interaction of various types of immune cells and signaling pathways between  
53 the tumor and immune cells[12]. There are several kinds of immunotherapy to treat BC, such as  
54 intravesical administration of the Bacillus Calmette-Guerin vaccine for treating high-risk no-muscle  
55 invasive bladder cancer (NMIBC) [13]. Patient prognosis and treatment response were predicted by  
56 immune cells with current molecular stratification in patients with BC[14].

57 In this study, we divided BC into three distinct subtypes based on immune cell-related  
58 methylation sites profiles. The three methylation sites subtypes are related to different molecular  
59 features, cellular characteristics, and clinical results. The classification of immune-related  
60 methylation sites subtypes may promote the optimal scheme of BC patients responsive to  
61 immunotherapy.

## 62 **2. Results**

### 63 *2.1 Three subgroups based on Differentially methylation sites (DMSs)*

64 Seven hundred and eighty-two immune cell biomarker-associated genes were selected from  
65 previous studies, and corresponding 8703 immune cell biomarker-associated methylation sites were  
66 acquired. By Parameter of infiltration was adjusted P-value < 0.05 and  $|\Delta\text{beta}| > 0.2$ , 715  
67 Differentially methylation sites (DMSs) between normal samples and tumor samples were identified  
68 (Fig. 1A).



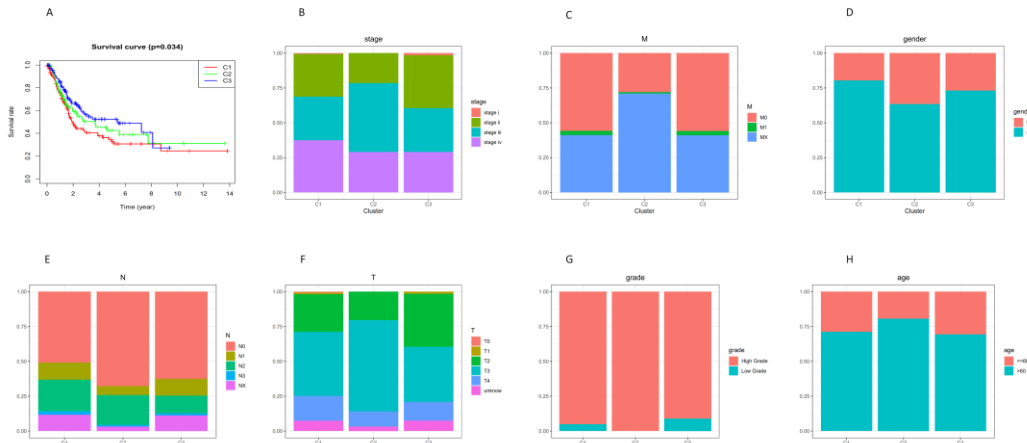
69

70 **Figure 1.** A. 715 Differentially methylation sites (DMSs) between normal samples and bladder cancer  
 71 samples. 1B.The consensus clustering of 715 Differentially methylation sites (DMSs) was divided into  
 72 three CpGs subgroups. B.The heatmap of methylation based on 715 Differentially methylation sites  
 73 (DMSs). C.Principal component analysis (PCA) validated the stability of classification.

74 *2.2. Classification of methylation subtypes of BC*

75 The consensus clustering of 715 DMSs was classified into three subtypes(Fig. 1B). Cluster 1  
 76 showed middle-methylation. Cluster 2 showed hyper-methylation. And cluster 3 showed hypo-  
 77 methylation (Fig. 1C). Principal component analysis (PCA) was utilized to check the stability of the  
 78 consensus classification(Fig. 1D) .

79 The overall survival (OS) curve of BC subsets was gotten with Kaplan–Meier method (Fig. 2A).  
 80 Cluster 1 had the worst prognosis. Cluster 3 had the best prognosis. A barplot showed the  
 81 relationship between clinical traits and the biological characteristics of subtypes.(Fig. 2.B-H). Based  
 82 on our results, Cluster 3 had more stage I, more low grade, and less T3.

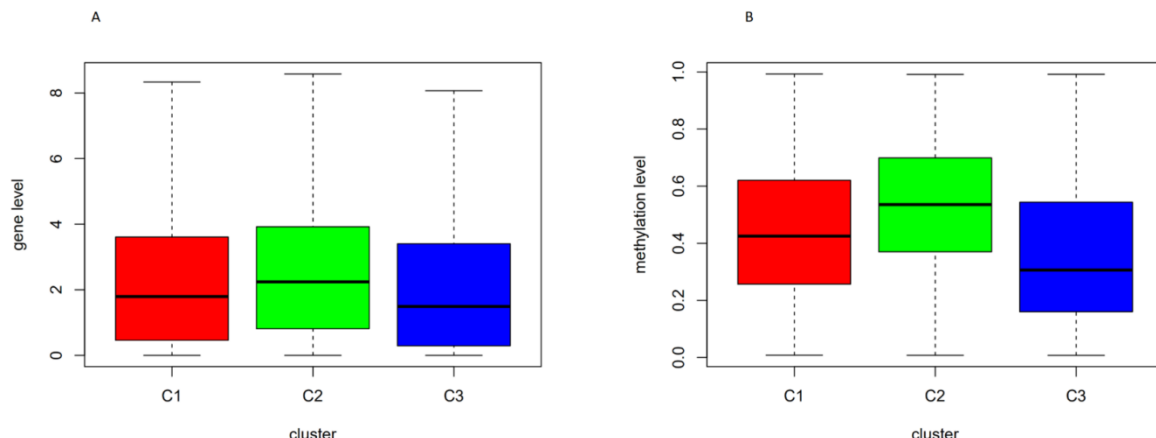


83

84 **Figure 2.** A.Overall survival (OS) curve. B-H. Clinicopathologic features among the three  
85 subgroups.

86 **2.3. Identifying different methylation level and distinct gene expression level of different subgroups**

87 Differentially immune cell biomarker-associated methylation levels was shown in Fig. 3B.  
88 Cluster 1 revealed middle-methylation. Cluster 2 revealed hyper-methylation. And cluster 3 revealed  
89 hypo-methylation. It was consistent with Fig 1C.



90

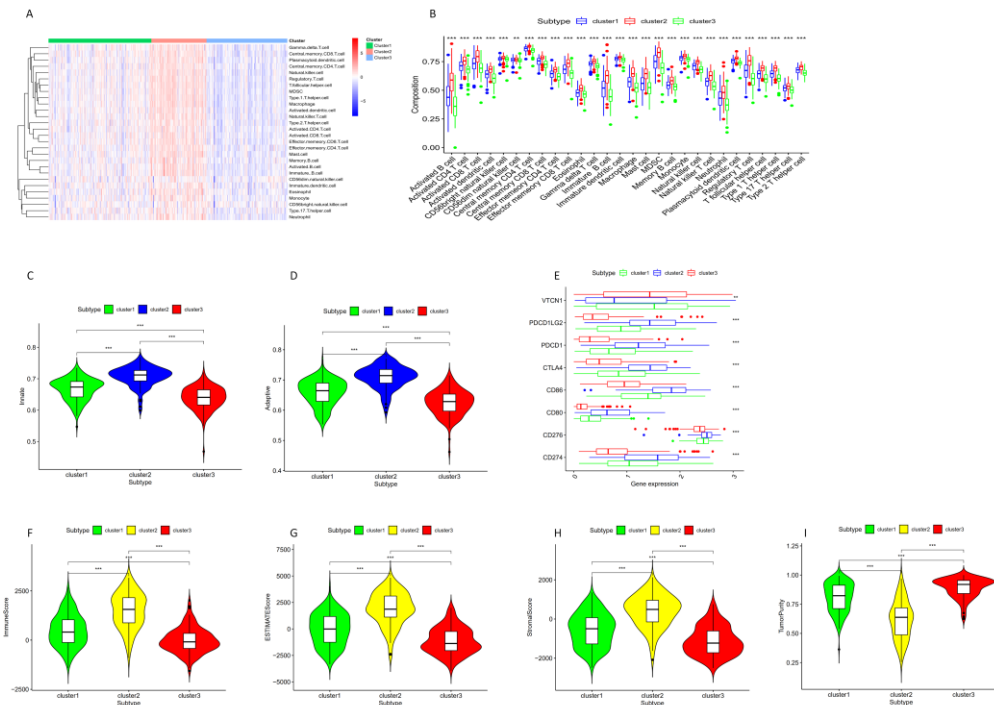
91 **Figure 3.** A. Gene level among the three subgroups. 3B. Methylation level among the three subgroups.

92 A previous study reported that the correlation between DNA methylation and gene expression  
93 in lung cancer was identified for about 750 genes. They found one-third of these correlations were  
94 positive, indicating the challenges in finding widespread and strong negative correlations between  
95 gene expression and genome-wide CpG methylation[30]. In fig 3A, immune cell genes expression is  
96 a high expression in cluster 2, low expression in cluster 3, and middle expression in cluster1. In the  
97 present study, high methylation level had high gene expression level.

98 **2.4. Immune in different subgroups**

99 In Fig. 4A, cluster 1 had middle immune infiltration. Cluster 2 was a correlation with high  
100 immune infiltration, and cluster 3 had low immune infiltration. Immune infiltration was compared  
101 among the three subtypes, and there were remarkable differences among these subtypes (Fig. 4B).  
102 Immune checkpoints were also significant differences among these subtypes (Figure 4E). Three

103 asterisks are P-value < 0.001. Two asterisks are P-value < 0.01. One asterisk is P-value < 0.05. Ns means  
 104 that there is no significance.



105

106 **Figure 4.** A. Immune cells infiltration among the three subtype. B. Immune cells the among three  
 107 subgroups. C-D. Innate immune cells and adaptive immune cells among the three subgroups.  
 108 E. Immune checkpoints among the three subsets. F-I. Immune microenvironment among the three  
 109 groups.

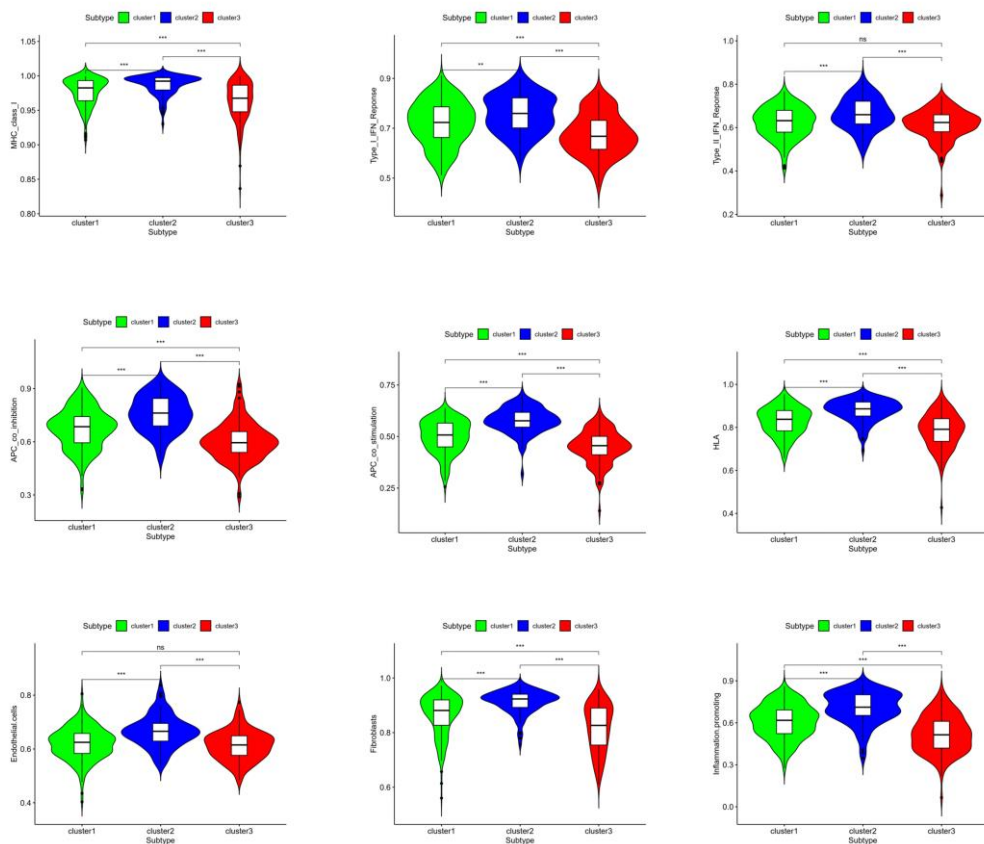
110 Three asterisks are P-value less than 0.001. Two asterisks are P-value less than 0.01. One  
 111 asterisk is P-value less than 0.05. Ns means that there is no significance

## 112 2.5. Tumor microenvironment (TME)

113 The tumor microenvironment contains stromal cells, tumor cells, and immune cells. The higher  
 114 stromal score and immune score, the lower purity of tumor. In Fig4.F-I, cluster 2 had the highest  
 115 stromal score, immune score, ESTIMATEScore, and the lowest purity of tumor. Cluster 3 had the  
 116 lowest stromal score, immune score, ESTIMATEScore, and the highest tumor purity.

## 117 2.6. Single sample gene set enrichment analysis (ssGSEA)

118 The bio-marker of APC\_co\_inhibition, APC\_co\_stimulation, Endothelial cells, Fibroblasts, HLA,  
 119 Inflammation-promoting, MHC\_class\_I, Type\_I\_IFN\_Reponse, and Type\_II\_IFN\_Reponse were  
 120 significantly different among these subtypes (Figure 5).

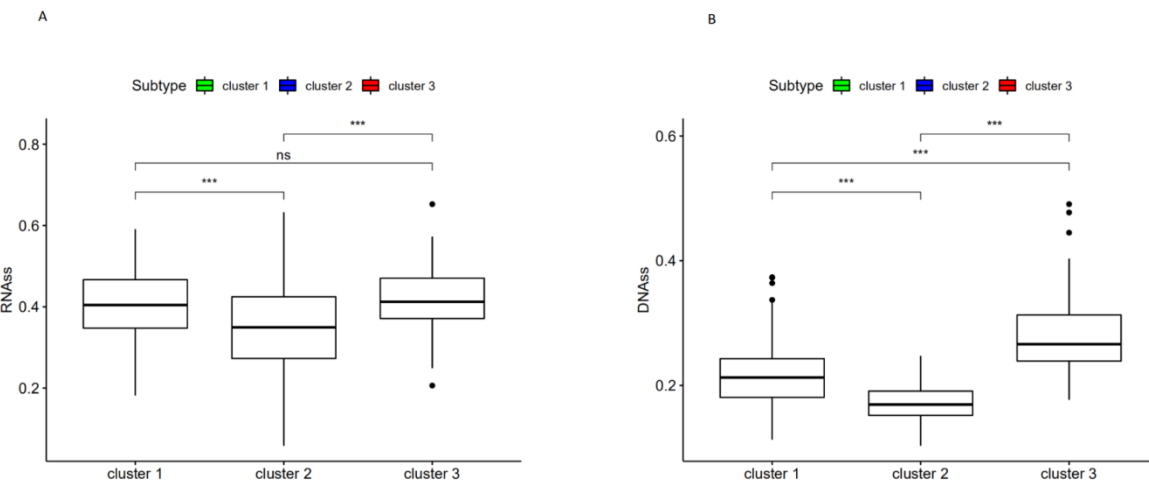


121

122 **Figure 5.** APC\_co\_inhibition, APC\_co\_stimulation, Endothelial cells, Fibroblasts, HLA,  
 123 Inflammation-promoting, MHC\_class\_I, Type\_I\_IFN\_Respons and Type\_II\_IFN\_Respons among the  
 124 three subgroups.

125 **2.7. DNA-methylation (DNAss) and mRNA (RNAss) among subgroups**

126 The DNA hypermethylation of those promoter genes suppressed gene expression, which in turn  
 127 benefited cancer cells. Therefore, down-regulation of those genes may lead to cancer stem and  
 128 progenitor cells' occurrence by DNA hypermethylation[24, 25]. RNA stemness score and DNA  
 129 stemness score were the lowest in cluster 2 in Fig.6.



130

131

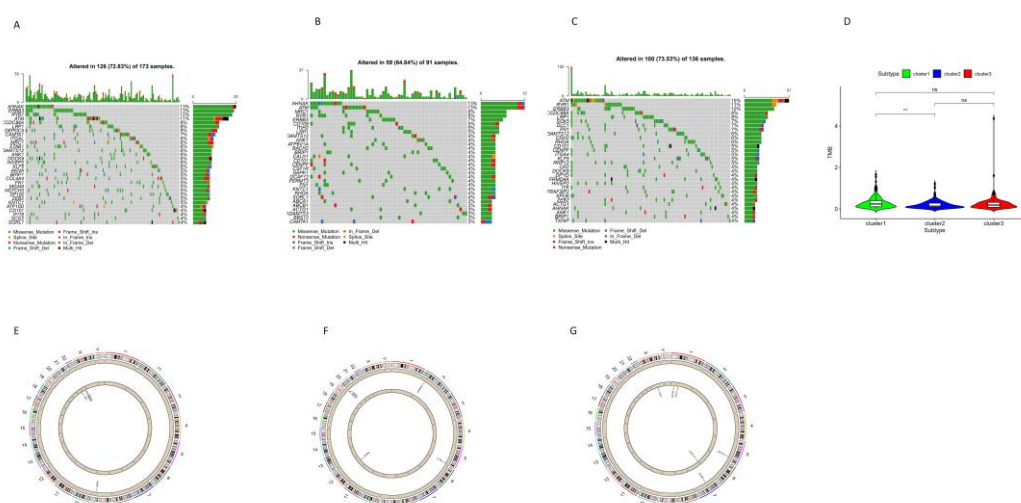
**Figure 6.** RNAss and DNAss among the three subgroups.

132

**2.8. Analysis of mutations and CNVs among three subgroups**

133

Thirty immune-cell-associated- genes with the highest mutation proportion in each subtype were shown in Fig. 7.A-C. And 58 immune-cell-associated- genes were identified from the above 30 genes in each subgroup. It meant that there was less overlap among the three subtypes (Fig. 7 A-C). The mutations of ITGA9, ENG, EVI5, ATIC, and FZD2 in cluster 1 were significantly higher than those in other subtypes. The mutations of CTSZ, HOXA1, and KLRF1 in cluster 2 were significantly higher than those in other subtypes. The mutations of DLC1, OSBPL1A, RRP12, C3AR1, MPZL1, and ITK in cluster 3 were significantly higher than those in other subtypes. TMB was a significant difference only between cluster 1 and cluster 2. TMB was a remarkable difference only between cluster 1 and cluster 2. (Fig. 7 D).



142

143

**Figure 7.** A. Immune cell genes-associated mutation in cluster1. B. Immune cell genes-associated mutation in cluster2. C. Immune cell genes-associated mutation mutation in cluster3. D. TMB among the three subtypes. E-G. Immune cell genes-associated CNVs in three subgroups, respectively.

144

Next, the CNV data was analyzed, 391 normal tissue and 410 tumor tissue were extracted. In figure 7E, CNV data in one subgroup was compared with the rest two subgroups. One gene with significant copy number gains was in cluster 1, and three genes with significant copy number losses were in cluster 1. Figure 7F showed four genes with significant copy number gains and one gene with significant copy number losses in cluster 2. In figure 7G, there were two genes with significant copy number gains and four genes with significant copy number losses in cluster 3.

152

**3. Discussion**

153

Altered DNA methylation patterns are hallmarks of tumors. Usually unmethylated promoters may alter into densely methylated, which will lead to the silencing of critical genes such as tumor suppressor genes[31]. Other sequences may alter into hypomethylated in tumors, which result in the abnormal activation of genes that are usually suppressed by DNA methylation[32]. Hypermethylation events have also been reported to be biomarkers of human tumors, for an early examination of blood, urine and other body fluids, for prognosis or prediction of response to treatment, and for monitoring cancer recurrence[33].

160

BC development is highly related to immune cell infiltration and inflammation. A previous study also revealed the interaction of various types of immune cells and signaling pathways between

162 the tumor and immune cells[12]. There are several kinds of immunotherapy to treat BC, such as  
163 intravesical administration of the Bacillus Calmette-Guerin vaccine for treating high-risk NMIBC  
164 [13]. Patient prognosis and treatment response were predicted by immune cells with current  
165 molecular stratification in patients with BC[14]. To understand the mechanism of cancer, guide  
166 therapy, and improve prognosis, it is vital for us to identify accurate subtypes. Several studies were  
167 reported to identify subtype based on DNA methylation, including colon adenocarcinoma[34],  
168 cervical cancer[35], glioblastoma[36], and bladder cancer[37]. This study divided BC into three  
169 distinct subtypes based on immune cells - related methylation profiles (Fig. 1B-C). To check for  
170 stability of the classification, PCA was utilized to validate the stability of the classification(Fig. 1D),  
171 and PCA proved the classification was stable and accurate. The three immune subtypes are related  
172 to significantly different clinical results(Fig. 2). The methylation levels among the three subtypes were  
173 different. Differentially immune cell biomarker-associated methylation level was shown in Fig. 1C.  
174 Cluster 1 revealed middle-methylation. Cluster 2 revealed hyper-methylation. And cluster 3 revealed  
175 hypo-methylation. This was consistent with Fig3B. The distribution of immune cells, level expression  
176 of checkpoints, stromal score, immune score, ESTIMATEScore, APC\_co\_inhibition,  
177 APC\_co\_stimulation, HLA, MHC\_class\_I, Type\_I\_IFN\_Reponse, and Type\_II\_IFN\_Reponse were  
178 significant difference among the three subgroups. All of those verified the stability and accuracy of  
179 the classification(Fig 4 and Fig 5).

180 In the present study, different subtypes had different survival. This may be caused by several  
181 reasons as followings. 1. Abnormal DNA methylation may lead to poor prognosis in cancer  
182 patients[38]. The progression and prognosis of cancer may be affected by Hyper-methylation of  
183 DNA[39]. 2. Tumor cells in the microenvironment can express high levels of immunosuppressive  
184 cytokines to forbid T cell proliferation and activity while facilitating tumor development and  
185 progression[40, 41]. Tumor-expressing specific molecular can be enough to induce  
186 immunosuppressive and facilitate immune evasion[42]. Subtle changes in the compositions of  
187 immune cells can have different influences on tumor progression[43]. Previous studies reported that  
188 a high density of macrophage in the microenvironment was correlated with poor prognosis of  
189 bladder cancer patients[44]. In our study, cluster 3 had good survival. In Fig 1C and Fig 4A, cluster 3  
190 showed the hypo-methylation and low immune cell infiltration. Hypo-methylation and low immune  
191 cell infiltration might be the reason that cluster 3 had good survival.

192 However, middle-methylation and middle immune infiltration were in cluster 1 that had the  
193 worst survival. Hyper-methylation and high immune infiltration were in cluster 2 that had  
194 intermediate survival. We may find the reason from checkpoints. VTCN1 expression up-regulation  
195 in bladder cancer led to worse survival[45, 46]. B7x (VTCN1 ) was remarkably overexpressed in many  
196 human cancers, and it repressed the antitumor immune effect and regulated to escape  
197 immunosurveillance[47] High-level expression of CD80 and CD86 may result in a good survival in  
198 patients with nasopharyngeal carcinoma[48]. The absence or low-level expression of CD80 and CD86  
199 in cancers may be one mechanism by which cancers escape immunosurveillance[48]. In fig.4E, these  
200 checkpoints were significant differences among the three subgroups. Among them, VTCN1 (B7-H4)  
201 was the higher expression in cluster 1. CD80 and CD86 were the lower expressions in cluster 1. So  
202 these may cause cluster 1 with worse survival than cluster 2.

203 The tumor microenvironment contains stromal cells, tumor cells, and immune cells. The higher  
204 stromal score and immune score, the lower purity of tumor. In Fig, cluster 2 had the highest stromal  
205 score, immune score, and the lowest tumor purity. Cluster 3 had the lowest stromal score, immune  
206 score, and the highest purity of the tumor. The distribution of immune score among three subgroups  
207 was consistent with the distribution of immune cells(Fig 4F-I).

208 Endothelial cells can remodel the local immune microenvironment and help tumor cells escape  
209 immunosurveillance in many ways[49]. Endothelial cells release chemokines to promote leukocyte  
210 migration into tumor tissues and express adhesion protein to facilitate peripheral leukocyte  
211 capture[50]. Endothelial cells can also forbid the activation and chemotaxis of immune cells and

212 mediate inhibitory molecules to facilitate immune tolerance[51, 52]. Endothelial cells also show  
213 increased expression of PD-L1 to repress T cell activation[53-55]. Besides, FasL expression in  
214 endothelial cells promotes their ability to suppress activation CD8+ T cells, causing endothelial cells-  
215 associated immune cell death and promote tumor escape[56, 57]. In the present study, the density of  
216 endothelial cells in cluster 2 was the highest, and immune infiltration was the highest in cluster2(Fig  
217 5). It inferred that the endothelial cells might help tumor cells escape immunity.

218 Cancer cells had interaction with cancer-associated macrophages and tumor-associated  
219 fibroblasts, which promotes tumor progression in bladder cancer[58]. In the present study, the  
220 distribution of fibroblasts among three subgroups was consistent with macrophages' distribution  
221 (Fig. 5). It suggested there was a correlation between fibroblasts and macrophages.

222 The patients in the therapy of tumors can benefit from the many inflammatory molecules that  
223 also have an important role in cancer progression and development. The dual role of inflammatory  
224 molecular is far from being fully understood[59]. In the present study, the distribution of  
225 inflammation-promoting among three subgroups was consistent with the distribution of immune  
226 cells(Fig.5). It indicated the inflammation-promoting and immune cells might affect each other. But  
227 the detailed role of inflammation-promoting may need more studies to be explored.

228 A previous study reported that the correlation between DNA methylation and gene expression  
229 in lung cancer was identified for about 750 genes. They found one-third of these the correlation was  
230 positive, indicating the challenges in finding widespread and strong negative correlations between  
231 genes expression and genome-wide CpG methylation[30]. In fig 3A, immune cell genes expression is  
232 a high expression in cluster 2, low expression in cluster 3, and middle expression in cluster1. It also  
233 challenged the finding widespread and strong negative correlations between genes expression and  
234 genome-wide CpG methylation.

235 The DNA hypermethylation of those promoter genes suppressed gene expression, which in turn  
236 benefited cancer cells. Therefore, down-regulation of those genes may lead to the occurrence of cancer  
237 stem and progenitor cells by DNA hypermethylation[24, 25]. The range of scores was from 0 to 1.  
238 Zero means high differentiation, and one means undifferentiation[26]. However, in the present study,  
239 RNA stemness score and DNA stemness score were the lowest in cluster 2 in Fig 6. It challenged the  
240 above findings which down-regulation of those genes may lead to the occurrence of cancer stem and  
241 progenitor cells by DNA hypermethylation. A previous study found that for several tumor types,  
242 such as BLCA, LUSC, HNSC, and GBM, there was a negative correlation between DNAss score with  
243 leukocyte fraction and/or lower PD-L1 expression[26]. In the present study, cluster 2 had the highest  
244 immune infiltration and high-level expression of CD274 (Fig.4E), but cluster 3 had the lowest DNAss  
245 score. This result was the same as the previous work. In present work, we also found the lower RNAss  
246 score was associated with higher immune infiltration and higher-level expression of CD274(Fig 6 and  
247 Fig. 4E).

248 TMB was a remarkable difference only between cluster 1 and cluster 2. (Fig. 7 D). It suggested  
249 the TMB might be not correlated with methylation level. But the composition of genes of mutations  
250 was different among the three subtypes. In Fig. 7. and 58 immune-cell-associated-genes were  
251 identified from the highest mutant 30 genes in each subgroup. It meant that there was less overlap  
252 among the three subtypes (Fig. 7 A-C). The mutations of ITGA9, ENG, EVI5, ATIC, and FZD2 in  
253 cluster 1 were significantly higher than those in other subtypes. These genes are the bio-marker of  
254 Mast cell, Plasmacytoid dendritic cell, Type 2 T helper cell, Immature dendritic cell, and  
255 Macrophage[15, 16]. The mutations of CTSZ, HOXA1, and KLRF1 in cluster 2 were significantly  
256 higher than those in rest subtypes. These genes are the bio-marker of Natural killer cell, CD56 bright  
257 natural killer cell, and Gamma delta T cell[15, 16]. The mutations of DLC1, OSBPL1A, RRP12, C3AR1,  
258 MPZL1, and ITK in cluster 3 were significantly higher than those in rest subtypes. These genes are  
259 the bio-marker of Type 2 T helper cell, Eosinophil, Effector memory CD8 T cell, Activated CD8 T  
260 cell, and Activated CD4 T cell[15, 16]. These immune cells with mutant genes among the three

261 subgroups were different. It is possible to become promising drug targets based on these mutant  
262 genes.

263 In figure 7E, CNV data in one subgroup was compared with the rest two subgroups. AKNA  
264 with significant copy number gains was in cluster 1 and the gene is the biomarker of Activated B  
265 cell[15, 16]. PARVG, SIK1 and UPK3A with significant copy number losses were in cluster 1 and these  
266 genes are the biomarker of MDSC, Effector memory CD8 T cell, and Monocyte[15, 16]. Figure 7F  
267 showed CLTB, GEMIN6, SIRPA and SIRPG with significant copy number gains. These genes are the  
268 biomarker of Immature dendritic cell, Activated CD8 T cell, Plasmacytoid dendritic cell, and Central  
269 memory CD4 T cell[15, 16]. DYRK2 with significant copy number losses was in cluster 2 and the gene  
270 is the biomarker of CD56 dim natural killer cell[15, 16]. In figure 7G, CSF1R and GUSB with  
271 significant copy number gains were in cluster 3 and these genes are the biomarker of T follicular  
272 helper cell and Central memory CD8 T cell[15, 16]. CDC7, CHST12, CSF3R and OGT with significant  
273 copy number losses were in cluster 3. These genes are the biomarker of Type 2 T helper cell, T  
274 follicular helper cell, Immature dendritic cell and Plasmacytoid dendritic cell[15, 16]. These immune  
275 cells with mutant genes among the three subgroups were totally different. It also is possible to  
276 become promising drug targets based on these CNV genes.

277 In conclusion: The classification was accurate and stable. BC patients could be divided into three  
278 subtypes based on the immune cells-associated CpG sites. Specific biological signaling pathways,  
279 immune mechanisms, and genomic alterations were various among three subgroups. High-level  
280 immune infiltration was a correlation with high-level methylation. The lower RNAss score was  
281 associated with higher immune infiltration and higher-level expression of CD274.

## 282 4. Materials and Methods

### 283 4.1. Data pre-processing

284 Methylation data from Illumina Human Methylation 450 arrays was obtained from UCSC Xena  
285 and had 437 samples (<https://xenabrowser.net/datapages/>, 2020-07-15). DNA-methylation (DNAss),  
286 mRNA stemness (RNAss), RNA-sequencing data from 430 BC samples and clinical data also were  
287 downloaded from UCSC Xena website. The Masked Somatic Mutation data (MuTect2. Variant0. Maf)  
288 and the CNV data set (Masked Copy Number Segment, affymetrix snp 6.0) were obtained from  
289 TCGA website (<https://portal.gdc.cancer.gov/repository>). The CNV data was comprised of 814  
290 samples. Because the databases were the public databases, and our data was obtained directly from  
291 these databases. There was no requirement for ethical approval.

### 292 4.2. Immune cells-associated genes selection

293 Immune cells-associated bio-markers were obtained from previous studies[15, 16]. And their  
294 corresponding methylation sites were obtained. The criteria for exclusion probes from the analysis  
295 was as followings: 1. If the CpG site data missed more than 70% in the samples, the CpG sites were  
296 excluded from the analysis[17]. 2. Cross-reactive genome CpG sites were deleted. 3. Probes on the X  
297 and Y chromosomes were moved excluded from the analysis. The remaining sites were imputed with  
298 the k-nearest neighbors (KNN) imputation procedure[18].

### 299 4.3. Unsupervised hierarchical cluster analysis

300 The methylation sites corresponding to immune cells-associated genes were acquired.  
301 Differentially methylation sites (DMSs) were identified between normal samples and bladder cancer  
302 samples with adjusted P-value < 0.05 and  $|\Delta\text{beta}| > 0.2$ . Unsupervised hierarchical clustering was  
303 performed based on immune cell-associated methylation data to identify subtypes of BC with  
304 “sparcl” R software package. The overall survival (OS) curve of BC subsets was gotten with Kaplan-  
305 Meier method and with “survival” package in R software. Principal component analysis (PCA) was

306 performed to validate the classification. A barplot showed the relationship between clinical traits and  
307 the biological characteristics of subtypes.

308 *4.4. Single sample gene set enrichment analysis (ssGSEA) based on immune cells bio-marker*

309 Single sample gene set enrichment analysis was performed to quantify the infiltration of  
310 immune cells. The ssGSEA ranked the genes based on their absolute expression in a sample with  
311 "GSEABase" and "GSVA" R package. The enrichment score is calculated by integrating the  
312 differences between the empirical cumulative distribution functions of the gene ranks[19, 20].  
313 Activated B cell, activated CD8 T cell, effector memory CD8 T cell, central memory CD8 T cell,  
314 activated CD4 T cell, effector memory CD4 T cell, central memory CD4 T cell, regulatory T cell,  
315 gamma delta T cell, immature B cell, memory B cell, type 17 T helper cell, T follicular helper cell, type  
316 1 T helper cell, and type 2 T helper cell are adaptive immune cells. CD56 dim natural killer cell, CD56  
317 bright natural killer cell, Eosinophil, Activated dendritic cell, Immature dendritic cell, MDSC,  
318 Macrophage, Monocyte, Mast cell, Plasmacytoid dendritic cell, Natural killer cell, Natural killer T  
319 cell, and Neutrophil are innate immune cells.

320 Immune checkpoints were selected from previous studies[21, 22] to be compared among the  
321 subtypes. Kruskal-Wallis Test was performed.

322 *4.5. Tumor microenvironment (TME)*

323 ESTIMATE algorithm was obtained from the public source website (<https://sourceforge.net/projects/estimateproject/>) to estimate the scores of stromal and immune cells based on gene  
324 expression signature in tumor samples. Then, we calculated stromal scores, immune scores, tumor  
325 purity, and ESTIMATE scores for each sample. Stromal scores, immune scores, tumor purity, and  
326 ESTIMATE scores were compared among subtypes.

328 *4.6. Single sample gene set enrichment analysis (ssGSEA)*

329 The bio-marker of APC\_co\_inhibition, APC\_co\_stimulation, Endothelial cells, Fibroblasts, HLA,  
330 Inflammation-promoting, MHC\_class\_I, Type\_I\_IFN\_Reponse and Type\_II\_IFN\_Reponse were  
331 selected from studies[19, 20]. Single sample gene set enrichment analysis was performed to rank the  
332 genes based on their absolute expression in a sample.

333 *4.7. DNA-methylation (DNAss) and mRNA stemness (RNAss) among subgroups*

334 During cancer progression, a differentiated phenotype was lost, and progenitor and stem-cell-  
335 like characteristics were acquired[23]. The DNA hypermethylation of those genes suppressed gene  
336 expression, which in turn benefited cancer cells. Therefore, down-regulation of those genes may lead  
337 to the occurrence of cancer stem and progenitor cells by DNA hypermethylation[24, 25]. RNA  
338 stemness score based on mRNA expression (RNAss) and DNA stemness score based on DNA  
339 methylation pattern (DNAss) were utilized to measure tumor stemness[26]. The range of scores was  
340 from 0 to 1. Zero means high differentiation, and 1 means undifferentiation[26]. DNA-methylation  
341 (DNAss) and mRNA (RNAss) among three subgroups were analyzed.

342 *4.8. Analysis of mutations and CNVs among subgroups.*

343 The 'maftools' software package was utilized to analyze and visualize immune cell biomarker-  
344 associated mutation data[27]. Immune cell biomarker-associated mutation data was compared  
345 between one group with the rest groups with Chi-square Test. The P-value is less than 0.05. TMB is  
346 called the density of tumor genes mutation[27]. TMB (tumor mutation burden) was compared among  
347 subtypes based on immune cell biomarker-associated mutation data.

348 Then, immune cell biomarker-associated CNV data was analyzed. Genomic identification of  
349 significant targets in cancer (GISTIC) algorithm was utilized to classify the copy number variant

350 genes with remarkable gains and losses[28, 29]. Parameter thresholds were set to 0.2 and -0.2 for  
351 genomic gains and losses, respectively[28, 29]. Immune cell biomarker-associated copy number  
352 variant data was compared between one group with the rest groups with a Chi-square Test and P-  
353 value < 0.01.

354 **5. Conclusions**

355 The classification was accurate and stable. BC patients could be divided into three subtypes  
356 based on the immune cells-associated CpG sites. Specific biological signaling pathways, immune  
357 mechanisms, and genomic alterations were various among three subgroups. High-level immune  
358 infiltration was a correlation with high-level methylation. The lower RNAss score was associated  
359 with higher immune infiltration and higher-level expression of CD274.

360 **Author Contributions:** conception and design: All authors. Data analysis and interpretation: Qizhan Luo.  
361 Manuscript writing: Qizhan Luo. Final approval of manuscript: All authors

362 **Funding:** China Scholarship Council

363 **Conflicts of Interest:** The authors declare that they have no competing interests.

364 **Data available:** Our data was gotten directly from public databases and the publishing policies of these  
365 databases were strictly obeyed by us, and there was no requirement for ethical approvals.

366 **References**

- 367 1. Del, P.J., Immunotherapy: Cancer immunotherapy and the value of cure. *Nat Rev Clin Oncol*, 2018. 15(5):  
368 p. 268-270.
- 369 2. Christofi, T., et al., Current Perspectives in Cancer Immunotherapy. *Cancers (Basel)*, 2019. 11(10).
- 370 3. Le DT, et al., PD-1 Blockade in Tumors with Mismatch-Repair Deficiency. *N Engl J Med*, 2015. 372(26): p.  
371 2509-20.
- 372 4. Reck, M., et al., Pembrolizumab versus Chemotherapy for PD-L1-Positive Non-Small-Cell Lung Cancer. *N  
373 Engl J Med*, 2016. 375(19): p. 1823-1833.
- 374 5. Wolchok, J.D., et al., Nivolumab plus ipilimumab in advanced melanoma. *N Engl J Med*, 2013. 369(2): p.  
375 122-33.
- 376 6. Mirjacic, M.K., et al., Attenuated in vitro effects of IFN-alpha, IL-2 and IL-12 on functional and receptor  
377 characteristics of peripheral blood lymphocytes in metastatic melanoma patients. *Cytokine*, 2017. 96: p. 30-  
378 40.
- 379 7. Chemin, I., Evaluation of a hepatitis B vaccination program in Taiwan: impact on hepatocellular carcinoma  
380 development. *Future Oncol*, 2010. 6(1): p. 21-3.
- 381 8. Mamasas, I.N., et al., Vaccination against human papilloma virus (HPV): epidemiological evidence of HPV  
382 in non-genital cancers. *Pathol Oncol Res*, 2011. 17(1): p. 103-19.
- 383 9. Kantoff, P.W., et al., Sipuleucel-T immunotherapy for castration-resistant prostate cancer. *N Engl J Med*,  
384 2010. 363(5): p. 411-22.
- 385 10. Le DT, et al., Safety and survival with GVAX pancreas prime and Listeria Monocytogenes-expressing  
386 mesothelin (CRS-207) boost vaccines for metastatic pancreatic cancer. *J Clin Oncol*, 2015. 33(12): p. 1325-33.
- 387 11. Christofi, T., et al., Current Perspectives in Cancer Immunotherapy. *Cancers (Basel)*, 2019. 11(10).
- 388 12. Masson-Lecomte, A., et al., Inflammatory biomarkers and bladder cancer prognosis: a systematic review.  
389 *Eur Urol*, 2014. 66(6): p. 1078-91.

390 13. Kawai, K., et al., Bacillus Calmette-Guerin (BCG) immunotherapy for bladder cancer: current  
391 understanding and perspectives on engineered BCG vaccine. *Cancer Sci*, 2013. 104(1): p. 22-7.

392 14. Wang, Y., et al., Prognostic value of immune cell infiltration in bladder cancer: A gene expression-based  
393 study. *Oncol Lett*, 2020. 20(2): p. 1677-1684.

394 15. Charoentong, P., et al., Pan-cancer Immunogenomic Analyses Reveal Genotype-Immunophenotype  
395 Relationships and Predictors of Response to Checkpoint Blockade. *Cell Rep*, 2017. 18(1): p. 248-262.

396 16. Xiao, Y., et al., Multi-Omics Profiling Reveals Distinct Microenvironment Characterization and Suggests  
397 Immune Escape Mechanisms of Triple-Negative Breast Cancer. *Clin Cancer Res*, 2019. 25(16): p. 5002-5014.

398 17. Li, C., et al., DNA methylation data-based molecular subtype classification related to the prognosis of  
399 patients with cervical cancer. *J Cell Biochem*, 2020. 121(3): p. 2713-2724.

400 18. Yang, C., et al., Molecular subtypes based on DNA methylation predict prognosis in colon adenocarcinoma  
401 patients. *Aging (Albany NY)*, 2019. 11(24): p. 11880-11892.

402 19. Finotello, F. and Z. Trajanoski, Quantifying tumor-infiltrating immune cells from transcriptomics data.  
403 *Cancer Immunol Immunother*, 2018. 67(7): p. 1031-1040.

404 20. Bindea, G., et al., Spatiotemporal dynamics of intratumoral immune cells reveal the immune landscape in  
405 human cancer. *Immunity*, 2013. 39(4): p. 782-95.

406 21. Zheng, M., et al., Identification of immune-enhanced molecular subtype associated with BRCA1 mutations,  
407 immune checkpoints and clinical outcome in ovarian carcinoma. *J Cell Mol Med*, 2020. 24(5): p. 2819-2831.

408 22. Li, W., et al., Multi-omics Analysis of Microenvironment Characteristics and Immune Escape Mechanisms  
409 of Hepatocellular Carcinoma. *Front Oncol*, 2019. 9: p. 1019.

410 23. Zhang, X., et al., A pan-cancer study of class-3 semaphorins as therapeutic targets in cancer. *BMC Med  
411 Genomics*, 2020. 13(Suppl 5): p. 45.

412 24. Ohm, J.E., et al., A stem cell-like chromatin pattern may predispose tumor suppressor genes to DNA  
413 hypermethylation and heritable silencing. *Nat Genet*, 2007. 39(2): p. 237-42.

414 25. Jones, P.A. and S.B. Baylin, The epigenomics of cancer. *Cell*, 2007. 128(4): p. 683-92.

415 26. Malta, T.M., et al., Machine Learning Identifies Stemness Features Associated with Oncogenic  
416 Dedifferentiation. *Cell*, 2018. 173(2): p. 338-354.e15.

417 27. Lv, J., et al., Mining TCGA database for tumor mutation burden and their clinical significance in bladder  
418 cancer. *Biosci Rep*, 2020. 40(4).

419 28. Yang, J., et al., The Landscape of Somatic Copy Number Alterations in Head and Neck Squamous Cell  
420 Carcinoma. *Front Oncol*, 2020. 10: p. 321.

421 29. Luo, H., et al., Genome-wide somatic copy number alteration analysis and database construction for  
422 cervical cancer. *Mol Genet Genomics*, 2020. 295(3): p. 765-773.

423 30. Long, M.D., D.J. Smiraglia and M.J. Campbell, The Genomic Impact of DNA CpG Methylation on Gene  
424 Expression; Relationships in Prostate Cancer. *Biomolecules*, 2017. 7(1).

425 31. Jones, P.A. and S.B. Baylin, The epigenomics of cancer. *Cell*, 2007. 128(4): p. 683-92.

426 32. Feinberg, A.P., Phenotypic plasticity and the epigenetics of human disease. *Nature*, 2007. 447(7143): p. 433-  
427 40.

428 33. Laird, P.W., The power and the promise of DNA methylation markers. *Nat Rev Cancer*, 2003. 3(4): p. 253-  
429 66.

430 34. Yang, C., et al., Molecular subtypes based on DNA methylation predict prognosis in colon adenocarcinoma  
431 patients. *Aging (Albany NY)*, 2019. 11(24): p. 11880-11892.

432 35. Yang, S., et al., HPV-related methylation-based reclassification and risk stratification of cervical cancer. *Mol*  
433 *Oncol*, 2020.

434 36. Noushmehr, H., et al., Identification of a CpG island methylator phenotype that defines a distinct subgroup  
435 of glioma. *Cancer Cell*, 2010. 17(5): p. 510-22.

436 37. Tian, Z., et al., DNA methylation-based classification and identification of bladder cancer prognosis-  
437 associated subgroups. *Cancer Cell Int*, 2020. 20: p. 255.

438 38. Hao, X., et al., DNA methylation markers for diagnosis and prognosis of common cancers. *Proc Natl Acad*  
439 *Sci U S A*, 2017. 114(28): p. 7414-7419.

440 39. Arai, E. and Y. Kanai, Genetic and epigenetic alterations during renal carcinogenesis. *Int J Clin Exp Pathol*,  
441 2010. 4(1): p. 58-73.

442 40. Chakraborty, S., et al., Transcriptional regulation of FOXP3 requires integrated activation of both promoter  
443 and CNS regions in tumor-induced CD8(+) Treg cells. *Sci Rep*, 2017. 7(1): p. 1628.

444 41. Chen, J., et al., Dendritic cells engineered to secrete anti-DcR3 antibody augment cytotoxic T lymphocyte  
445 response against pancreatic cancer in vitro. *World J Gastroenterol*, 2017. 23(5): p. 817-829.

446 42. Medina, P.J. and V.R. Adams, PD-1 Pathway Inhibitors: Immuno-Oncology Agents for Restoring  
447 Antitumor Immune Responses. *Pharmacotherapy*, 2016. 36(3): p. 317-34.

448 43. Pan, S., et al., Bladder Cancer Exhibiting High Immune Infiltration Shows the Lowest Response Rate to  
449 Immune Checkpoint Inhibitors. *Front Oncol*, 2019. 9: p. 1101.

450 44. Hu, B., et al., Blockade of DC-SIGN(+) Tumor-Associated Macrophages Reactivates Antitumor Immunity  
451 and Improves Immunotherapy in Muscle-Invasive Bladder Cancer. *Cancer Res*, 2020. 80(8): p. 1707-1719.

452 45. Podojil, J.R., et al., Antibody targeting of B7-H4 enhances the immune response in urothelial carcinoma.  
453 *Oncoimmunology*, 2020. 9(1): p. 1744897.

454 46. Fan, M., et al., B7-H4 expression is correlated with tumor progression and clinical outcome in urothelial  
455 cell carcinoma. *Int J Clin Exp Pathol*, 2014. 7(10): p. 6768-75.

456 47. John, P., et al., The B7x Immune Checkpoint Pathway: From Discovery to Clinical Trial. *Trends Pharmacol*  
457 *Sci*, 2019. 40(11): p. 883-896.

458 48. Chang, C.S., et al., Expression of CD80 and CD86 costimulatory molecules are potential markers for better  
459 survival in nasopharyngeal carcinoma. *BMC Cancer*, 2007. 7: p. 88.

460 49. Chen, W.Z., et al., Endothelial cells in colorectal cancer. *World J Gastrointest Oncol*, 2019. 11(11): p. 946-  
461 956.

462 50. Tilki, D., et al., Zone-specific remodeling of tumor blood vessels affects tumor growth. *Cancer*, 2007.  
463 110(10): p. 2347-62.

464 51. Folkman, J., Tumor angiogenesis: therapeutic implications. *N Engl J Med*, 1971. 285(21): p. 1182-6.

465 52. Ager, A., et al., Homing to solid cancers: a vascular checkpoint in adoptive cell therapy using CAR T-cells.  
466 *Biochem Soc Trans*, 2016. 44(2): p. 377-85.

467 53. Bichsel, C.A., et al., Increased PD-L1 expression and IL-6 secretion characterize human lung tumor-derived  
468 perivascular-like cells that promote vascular leakage in a perfusable microvasculature model. *Sci Rep*, 2017.  
469 7(1): p. 10636.

470 54. Jennewein, L., et al., Increased tumor vascularization is associated with the amount of immune competent  
471 PD-1 positive cells in testicular germ cell tumors. *Oncol Lett*, 2018. 15(6): p. 9852-9860.

472 55. Bagaria, S.P., et al., Association Between Programmed Death-Ligand 1 Expression and the Vascular  
473 Endothelial Growth Factor Pathway in Angiosarcoma. *Front Oncol*, 2018. 8: p. 71.

474 56. Motz, G.T., et al., Tumor endothelium FasL establishes a selective immune barrier promoting tolerance in  
475 tumors. *Nat Med*, 2014. 20(6): p. 607-15.

476 57. Hendrix, M.J., et al., Vasculogenic mimicry and tumour-cell plasticity: lessons from melanoma. *Nat Rev  
477 Cancer*, 2003. 3(6): p. 411-21.

478 58. Miyake, M., et al., CXCL1-Mediated Interaction of Cancer Cells with Tumor-Associated Macrophages and  
479 Cancer-Associated Fibroblasts Promotes Tumor Progression in Human Bladder Cancer. *Neoplasia*, 2016.  
480 18(10): p. 636-646.

481 59. Chow, M.T., A. Moller and M.J. Smyth, Inflammation and immune surveillance in cancer. *Semin Cancer  
482 Biol*, 2012. 22(1): p. 23-32.

483